IOP Conf. Series: Materials Science and Engineering **392** (2018) 062051 doi:10.1088/1757-899X/392/6/062051

A method to predict the cutting force for end mills with variable-pitch and variable-helix angle

G Jin[1], H Li[2], ZJ Li[1] and GX Sun[3]

[1]Tianjin Key Lab of High Speed Cutting and Precision Machining, Tianjin University of Technology and Education, Tianjin 300222, China

[2]Tianjin Jinhang Institute of Technical Physical, Tianjin 300300, China

[3]Tianjin BAOLAI Group, Tianjin 301809, China

Abstract. Cutting force is the most fundamental, and essential for machining error control, chatter stability analysis and milling process planning. In this paper, a method to predict the cutting force for the milling with variable-pitch or variable-helix cutter is provided. The method can take into account the piecewise continuous regions of the cutting that is attributed to the helix angle and the pitch variations between two subsequent teeth along the length of the axis. The piecewise character related to cutting force is deeply analysed and the effective depth of cut which seriously influences the maximum cutting force is discussed as well as its expression. Finally, a series of cutting tests and simulations are carried out to validate the present method.

1. Introduction

Milling is a very commonly used manufacturing process for machining metal components made of steel, aluminum alloy and titanium alloy in industry due to its versatility to generate complex shapes in variety of materials at high quality. As one of the most important part of this process, cutting force is the most fundamental, and essential for machining error control, chatter stability analysis and milling process planning. Koenigsberger and Sabberwal [1] developed one formula for milling forces using mechanistic modeling. Altintas [2] assumed that the chip shearing and flank edge rubbing mechanism can separately be modelled as a function of chip load and a function of chip width. To improve the prediction accuracy of the models with constant cutting force coefficients, models with instantaneous cutting force coefficients such as Weibull function in Ko et al. [3] and exponential function in Wan et al. [4] were proposed. The cutter with variable helix angle is effective in avoid milling chatter because of its disruption of regenerative effect. However, a review of the literature shows that although some related research efforts have focused on the milling process with the related cutter, such as the stability analysis of variable–pitch or –helix milling [5], the effect of helix angle variation [6] on milling stability and optimization of tool geometry [7], there has been very little work systematically and deeply investigated the cutting force of milling process with variable helix cutter.

The focus of the current manuscript is to theoretically and experimentally investigate the cutting force in milling process with respect to variable helix cutter. The work of this paper is organized as follows. Firstly, a new model is presented to predict the cutting force in this case. Then, related analysis is carried out and the proposed method was verified through comparisons with experimental tests. The final section describes the conclusions from this work.

2. Mathematical Model

2.1. Cutting forces model considering variable pitch and helix angle

A cutter with radius R and N unequally spaced teeth rotating at a constant velocity Ω (rev/min) is considered. For orthogonal directions x and y, if given the helix of the tool, the tangential and normal forces acting on a differential element of height dz can be written as:

$$\begin{pmatrix} F_x(t) \\ F_y(t) \end{pmatrix} = \begin{pmatrix} \sum_{j=1}^{N} \int_0^{a_p} -\mathrm{d}F_{tj}(t,z)\cos\phi_j(t,z) - \mathrm{d}F_{rj}(t,z)\sin\phi_j(t,z) \\ \sum_{j=1}^{N} \int_0^{a_p} \mathrm{d}F_{tj}(t,z)\sin\phi_j(t,z) - \mathrm{d}F_{rj}(t,z)\cos\phi_j(t,z) \end{pmatrix} \tag{1}$$

where a_p is the axial depth of cut, $\mathrm{d}F_{xj}(t,z)$ and $\mathrm{d}F_{yj}(t,z)$ are the differential forces. The tangential ($\mathrm{d}F_{tj}(t,z)$) and radial ($\mathrm{d}F_{rj}(t,z)$) differential cutting force components can be expressed as:

$$\begin{aligned} \mathrm{d}F_{tj}(t,z) &= g(\phi_j(t,z))(k_{tc}h_j(t,z) + k_{te})\mathrm{d}z \\ \mathrm{d}F_{rj}(t,z) &= g(\phi_j(t,z))(k_{rc}h_j(t,z) + k_{re})\mathrm{d}z \end{aligned} \tag{2}$$

Here, $g(\phi_j(t,z))$ denotes whether the *j*-th tooth is cutting. k_{tc} (k_{te}) and k_{rc} (k_{re}) are the linearized cutting (plough) force coefficients along the tangential and radial directions of the tool, respectively.

In order to facilitate analysis, two features are defined to characterize a certain variable helix tool, i.e., the pitch angle between (j, j−1) teeth at the tool tip ψ_{0j}, and the *j*-th helix angle of flute β_j. The angular position of *j*-th tooth is dependent on above two tool geometries and can be defined as

$$\phi_j(t,z) = \begin{cases} \dfrac{2\pi\Omega}{60}t - z\dfrac{\tan\beta_j}{R}, \text{if } j = 1 \\ \dfrac{2\pi\Omega}{60}t + \sum_{i=2}^{j}\psi_{0i} - z\dfrac{\tan\beta_j}{R}, \text{if } 1 < j \le N \end{cases} \tag{3}$$

The static chip thickness $h_j(t,z)$ can be expressed as

$$h_j(t,z) = f_t(\phi_j(t,z))\sin\phi_j(t,z) \tag{4}$$

where $f_t(\phi_j(t,z))$ defines the feed per tooth, and defined by

$$f_{tj}(t,\phi) = \frac{f_{t,mean}\cdot\psi_j(t,\phi)\cdot N}{2\pi} \tag{5}$$

where $\psi_j(t,\phi) = \psi_{0j} + \Delta\psi_j(t,\phi) = \psi_{0j} + (\phi_{j0}(t) - \phi)\alpha_j$, and $\alpha_j = (\tan\beta_1 - \tan\beta_N)/\tan\beta_1$ (for j=1) but $\alpha_j = (\tan\beta_j - \tan\beta_{j-1})/\tan\beta_j$ for $1 < j \le N$.

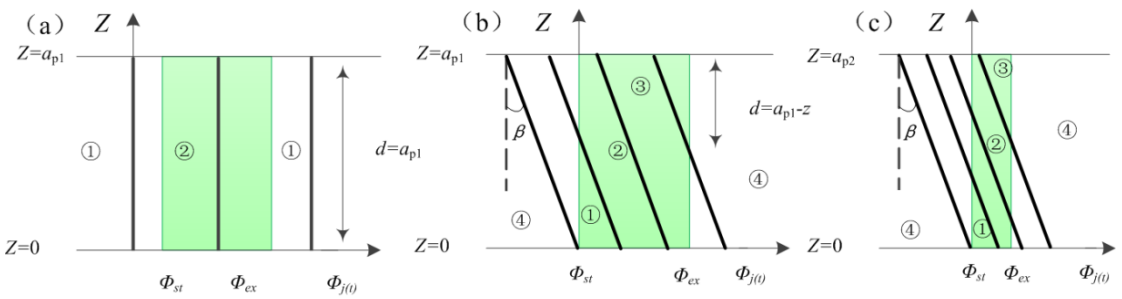

Figure 1. Schematic diagram of the three cutting regions, where the analytical force expression can be obtained. (a) Cutting with straight teeth cutter. (b) Helix angle cutter in big depth of cut. (c) Helix angle cutter in small depth of cut.`

Substituting equations (2), (3), (4), and (5) into equation (1) and considering $dz = -R/\tan\beta_j d\phi = -\varepsilon_j d\phi$ (i.e., $\varepsilon_j = R/\tan\beta_j$) from equation (4), the resulting expressions can be yield as

$$\boldsymbol{F}(t) = -\sum_{j=1}^{N} \varepsilon_j \int_{\phi_j(t,0)}^{\phi_j(t,a_p)} g(\phi)\left(f_{tj}(t,\phi)\boldsymbol{K}_1 + \boldsymbol{K}_2\right) d\phi \tag{6}$$

where $\boldsymbol{K}_1 = \begin{pmatrix} -k_{tc}\,\mathrm{c}\mathrm{s} - k_{rc}s^2 \\ k_{tc}\,\mathrm{s}^2 - k_{rc}\,\mathrm{cs} \end{pmatrix}$, $\boldsymbol{K}_2 = \begin{pmatrix} k_{te}\,\mathrm{s} - k_{re}c \\ -k_{te}\,\mathrm{c} - k_{re}s \end{pmatrix}$, $\mathrm{s} = \sin\phi_j(t,z), \mathrm{c} = \cos\phi_j(t,z)$

$\boldsymbol{F}(t)$ is piecewise continuous in the entry, middle-of-cut, and exit regions, as shown in figure 1. Definding $\mathbf{C} = (\phi_{sj}(t), \phi_{ej}(t))$, such that

$$\mathbf{C} = (\phi_{st\_j}(t), \phi_{ex\_j}(t)) \rightarrow \begin{cases} \phi_{st\_j}(t) = \max(\phi_j(t,a_p), \phi_{st}) \\ \phi_{ex\_j}(t) = \min(\phi_j(t,0), \phi_{ex}) \end{cases} \tag{7}$$

where

$$G(\phi_{0j}(t)) = \begin{cases} 1 & if \quad \phi_s < \phi_{0j}(t) < \phi_e + \phi_{lag,j} \\ 0 & otherwise \end{cases} \tag{8}$$

Where $\phi_{lag,j}$ is a function of helix angle β_j and axial depth of cut a_p, which is equal to $a_p * \tan(\beta_j)/R$. Substituting equations (7) and (8) into equation (6) yields

$$\boldsymbol{F}(t) = \sum_{j=1}^{N} G(\phi_{j0}(t))\varepsilon_j \int_{\phi_{js}(t)}^{\phi_{je}(t)} \left(f_{tj}(t,\phi)\boldsymbol{K}_1 + \boldsymbol{K}_2\right) d\phi \tag{9}$$

Equation (9) presents a unified cutting force expression suitable for any possible cutting region. Therefore, the calculation of the cutting force following different regions is unnecessary, thus benefitting application and programming.

3. Cutting force analysis

3.1. Effective depth of cut

When cutting with straight tooth cutter, the effective cutting depth is equal to a_{p1}. i.e., the cutting depth is big as shown in figure 1(a), only one point cutting occurs and the effective cutting depth equals 0; when the cutting depth increases from 0 to a_{p1}, the cutting tooth is in the case of process ①(see figure 1b). The maximum value is a_{p1} for any cutting position; for the process ②, the depth of cut has remained a_{p1} as well as the effective depth of cut; for the process ③, the effective depth of cut decreases from a_{p1} to 0. All in all, the effective cutting depth is segmented due to the presence of the tool helix angle β. From the above analysis, it can be obtained that at the small axial depth of cut, the effective depth of cut at arbitrary positions can be represented by

$$d_j(t)=\begin{cases}(\phi_j(t)-\phi_{st})R\tan^{-1}\beta, & \phi_{st}<\phi_j(t)<\phi_{st}+\phi_{lag}\\ a_p, \phi_{st}+\phi_{lag}<\phi_j(t)<\phi_{ex}\\ (a_p-(\phi_j(t)-\phi_{ex})R\tan^{-1}\beta, \phi_{ex}<\phi_j(t)<\phi_{ex}+\phi_{lag}\\ 0, \text{otherwise}\end{cases} \quad (10)$$

For the case of $\phi_{ex}-\phi_{st}<\phi_{lag}$, i.e., the cutting depth is small as shown in figure 1 (c), in the same way, the effective depth of cut can be expressed as

$$d_j(t)=\begin{cases}(\phi_j(t)-\phi_{\mathrm{st}})R\tan^{-1}\beta, & \phi_{\mathrm{st}}<\phi_j(t)<\phi_{\mathrm{ex}}\\ (\phi_{\mathrm{ex}}-\phi_{\mathrm{st}})R\tan^{-1}\beta, \phi_{\mathrm{ex}}<\phi_j(t)<\phi_{\mathrm{st}}+\phi_{\mathrm{lag}}\\ a_{\mathrm{p}}-(\phi_j(t)-\phi_{\mathrm{ex}})R\tan^{-1}\beta, & \phi_{\mathrm{st}}+\phi_{\mathrm{lag}}<\phi_j(t)<\phi_{\mathrm{ex}}+\phi_{\mathrm{lag}}\\ 0, \text{otherwise}\end{cases} \quad (11)$$

It can be seen from equation (11) that in the case of small axial depth of cut, the maximum effective depth of cut in the cutting process is not related to the axial depth a_p, in other words, when the maximum effective depth of cut is reached, and the cutting force is not increasing even if the axial depth a_p increased.

(1) Influence of helix angle to the cutting time

From figure 2(a) to 2(b), the axial depth of cut increases from 1mm to 10mm. For β = 0°, their cutting time does not change seriously. However, for β = 20° or 45°, the cutting time is increasing obviously as well as the depth of cut. This increases seemly correspond to the cutting time of processes ① and ③.

(2) Influence of helix angle to the maximum of cutting force

For the case of β=0°， as the depth of cut is increasing, the cutting time and shape of cutting force seemly keep unchanged, but the cutting force is increasing linearly. For β=20°, the piecewise continuous character of the cutting force is more and more clearly as the increasing of depth of cut. For β=45°, It can be clearly seen that the cutting force changes during the cutting process and the maximum cutting force is 50.94N. Comparing the maximum effective depth of cut and the maximum value of cutting force corresponding to β=20° and 45°, the tool traverses the entire cutting area, the maximum value of cutting force is independent of the cutting thickness, but is proportional to the maximum effective depth, i.e., $d_{\max}(\beta=20^o)/F_{\max}(\beta=20^o)=d_{\max}(\beta=45^o)/F_{\max}(\beta=45^o)$.

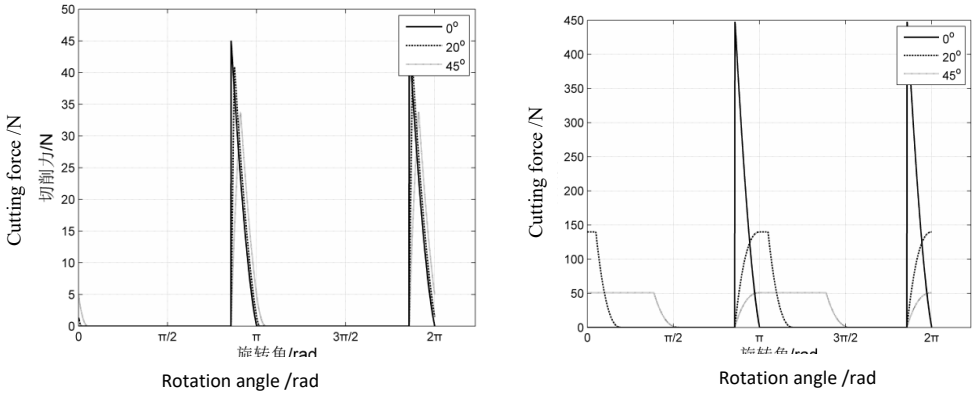

Figure 2. Cutting force in different depth of cut. (a) a_p=1mm; (b) a_p=10mm

3.2. Verification

To verify the effectiveness of the proposed approach on variable pitch and variable helix milling tools, Cutting force tests were conducted on a DMC 75 V linear five-axis high-speed machining center. Two

carbide end mills with R=12 mm, N=3 were used. These tools feature the same geometry except the tooth pitch at tool tip. The teeth of tool number **I** are regular cutter ($\boldsymbol{P}$ =[90,90,90]° and $\boldsymbol{\beta}$ =[30,30,30]°), while the tools number **II** are variable pitch cutters with $\boldsymbol{P}$ =[100,120,140]° and $\boldsymbol{\beta}=[30,35,35]^{\circ}$. The workpiece material was a block of aluminum alloy 6061-T651 with dimensions of 120×100×70 (mm) clamped on the Kistler dynamometer 9257B, which was adopted to measure the cutting force and was confined to the worktable. It can be seen from figure 3 that for each graph, very good consistency exists between the experimental and simulation results in X and Y directions in terms of magnitude, shape and phase width.

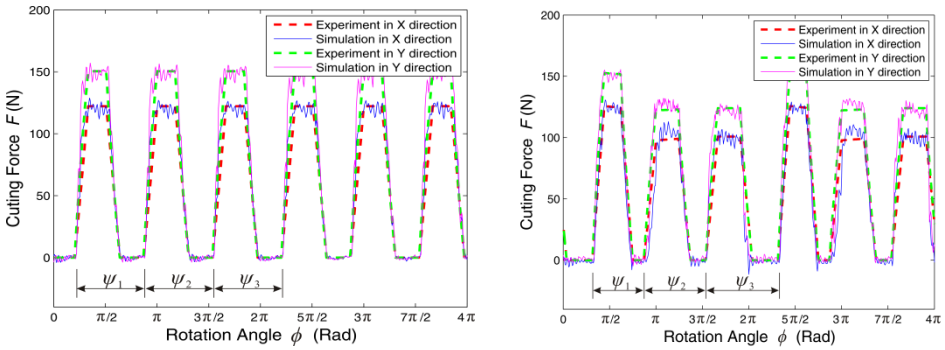

(a)Uniform-pitch cutter. (b) Variable-helix cutter with

Figure 3. Comparison of measured and predicted cutting forces in X and Y for different cutters.

4. Conclusions

In this paper, a method to predict the cutting force for the milling with variable-pitch or variable-helix cutter is provided. The method can take into account the piecewise continuous regions of the cutting that is attributed to the helix angle and the pitch variations between two subsequent teeth along the length of the axis. The piecewise character related to cutting force is deeply analysed and the effective depth of cut which influences the maximum cutting force is discussed as well as its expression. Finally, a series of cutting tests and simulations are carried out to validate the proposed method.

Acknowledgments

This work is supported by Innovation Team Training Plan of Tianjin Universities and colleges (Grant No. TD13-5096), National Natural Science Foundation of China (Grant No. 51405343), Key Projects in the Tianjin Science and Technology Pillar Program (Grant No. 17ZXZNGX00080).

References

[1] Koenigsberger F and Sabberwal AJP 1961 International Journal of Machine Tool Design and Research 1 15–33.
[2] Altintas Y and Budak E 1995 CIRP Ann-Manuf Techn 44 357 –62.
[3] Ko JH, Yun WS, Cho DW and Ehmann KF 2002 Int J Mach Tools Manuf 42 1595–605.
[4] Wan M, Zhang WH and Yang Y 2011 J Mater Process Tech 11 1852–63.
[5] Altintas Y, Engin S and Budak E 1999 J Manuf Sci Eng 121 173-8.
[6] Jin G, Zhang Q, Qi HJ and Yan B, 2014 P I MECH ENG C- Journal of Mechanical Engineering Science 228(15) 2702-10.
[7] Jin G, Qi HJ, Li ZJ and Han JX 2018 Commun Nonlinear Sci 63 38-56.